PHYSICAL REVIEW C VOLUME 11, NUMBER 5 MAY 1975

Complete fusion of heavy ions with ^{27}Al†

R. L. Kozub,* N. H. Lu, J. M. Miller, and D. Logan
Department of Chemistry, Columbia University, New York, New York 10027

T. W. Debiak
Department of Chemistry, State University of New York at Stony Brook, Stony Brook, New York 11794

L. Kowalski
Department of Physics, Montclair State College, Upper Montclair, New Jersey 07043
(Received 15 August 1974)

Cross sections for evaporation residues following complete fusion have been measured for the bombardment of ^{27}Al with 81-, 105-, 126-, and 168-MeV ^{16}O, 138- and 210-MeV ^{20}Ne, and 336-MeV ^{32}S. The results were obtained using a counter telescope and, in some cases, differ considerably from previous work with mica track detectors. The experimental critical angular momenta for fusion are in good agreement with recent theoretical calculations for the O and Ne bombardments. Our data suggest parameters for the critical distance of approach which are significantly smaller than previously reported values.

[NUCLEAR REACTIONS, COMPLETE FUSION $^{27}Al(^{16}O, {}^{43}Sc^*)$, $E=81$, 105, 126, 168 MeV; $^{27}Al(^{20}Ne, {}^{47}V^*)$, $E=138$, 210 MeV; $^{27}Al(^{32}S, {}^{59}Cu^*)$, $E=336$ MeV; measured $\sigma(\theta)$, σ for evaporation residues, deduced l_{cr}.]

I. INTRODUCTION

The dynamics of compound-nucleus formation in heavy ion reactions has been the subject of many experimental and theoretical investigations. Complete-fusion excitation functions can enhance our understanding of such reactions, although only a few such studies have been made previously with light nuclear systems.[1-3] In particular, complete-fusion cross sections for ^{16}O and ^{20}Ne bombardments of ^{27}Al were measured by Kowalski, Jodogne, and Miller[1] (KJM) using mica track detectors. In the present work, we repeat those experiments using a counter telescope. The cross section for the complete fusion of 336-MeV ^{32}S with ^{27}Al was also measured to complement the low-energy excitation function reported by Gutbrod, Winn, and Blann[3] (GWB) for this system. A portion of the present work has been reported elsewhere.[4]

II. EXPERIMENTAL METHOD AND RESULTS

A self-supporting ^{27}Al target of 147 $\mu g/cm^2$ thickness was bombarded with ^{16}O, ^{20}Ne, and ^{32}S ions from the Yale heavy ion accelerator. The reaction products were detected using a single-wire proportional counter (ΔE) and a Si surface barrier detector (E-ΔE). The ΔE detector has a Parylene C[5] window of thickness 0.31 μm and was operated with P-10 gas (90% Ar, 10% CH_4) at a nominal thickness of 200 $\mu g/cm^2$. The beam axis in the scattering chamber was located to within $\pm 0.2°$ by measuring cross sections for Rutherford scattering from Au on both sides of the beam. Pulses from the detectors were processed by conventional electronics and stored on magnetic tape by the PDP-8 computer in ΔE vs (E-ΔE) arrays. Data normalization was achieved by beam-current integration and by a monitor detector calibrated with the current integrator. The over-all normalization is accurate to about ±10%.

Elemental separation was clearly seen in the E vs (E-ΔE) array resulting from the reaction of 168-MeV $^{16}O+{}^{27}Al$. The heaviest events having velocities peaked near the velocity of the original compound nucleus were interpreted as evaporation residues following complete fusion. These were events with $Z \geq 10$ and $E \gtrsim 15$ MeV. Elemental ranges of $Z \geq 12$ and $Z \geq 18$ were used for evaporation residues in the Ne and S bombardments, respectively. The cross section for possible fission fragments in regions external to these was observed to be <10% of the evaporation residue cross section for $^{32}S+{}^{27}Al$, and an even smaller percentage for the Ne and O bombardments. High Z nuclei at energies $\lesssim 15$ MeV that were also observed are interpreted to be the heavy low-energy recoils from transfer reactions. A distinct separation between these recoils and the evaporation residues is evident in all our data, although not many of the recoils are observable at the lowest bombarding energies. Low-energy portions of the loci for some of the light transfer-reaction products are also observed.

Typical energy spectra for the evaporation residues are shown in Figs. 1–3. The peak positions and widths are consistent with those expected for evaporation residues having the Z distributions we observe, i.e., the residues are peaked at roughly the same velocity as the original compound nucleus. The spectra shown are for angles near the most probable angle of emission (i.e., the maximum of the $d\sigma/d\theta$ distribution). As expected,

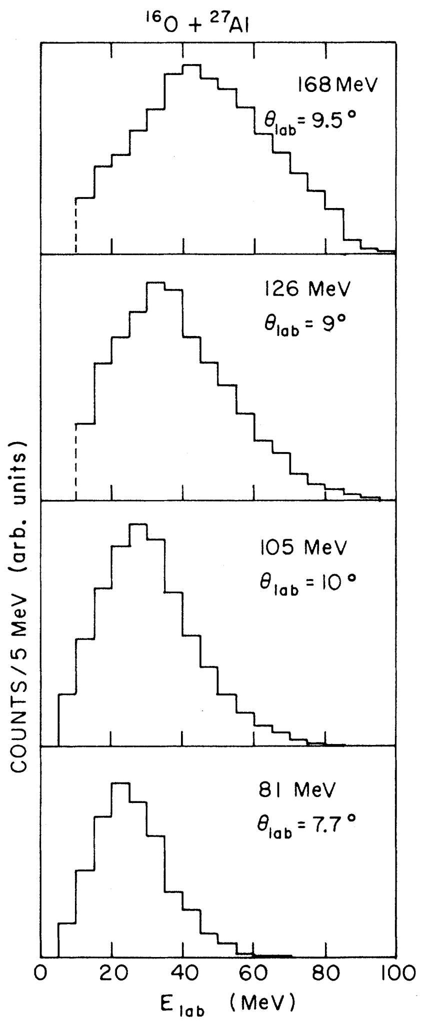

FIG. 1. Energy spectra for evaporation residues following complete fusion of ^{16}O and ^{27}Al. The laboratory angles are near the peaks in the $d\sigma/d\theta$ distributions. Dashed lines show the approximate point of division between evaporation residues and low-energy recoils from transfer reactions. The vertical scales are linear, and the maxima have from 500 to 2500 counts/5 MeV.

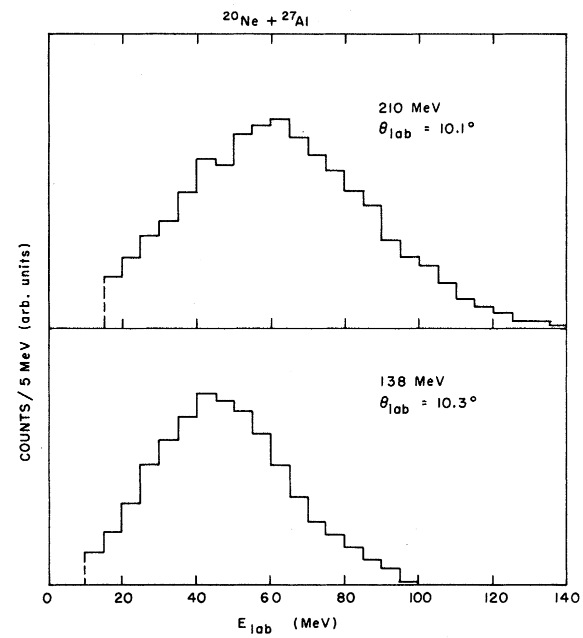

FIG. 2. Energy spectra for evaporation residues following complete fusion of ^{20}Ne and ^{27}Al. Peak heights are approximately 600 and 1000 counts/5 MeV for the 210- and 138-MeV data, respectively. (See also Fig. 1 caption.)

the peak position shifts to lower energies with increasing angle.

Angular distributions measured for the evaporation residues are shown in Figs. 4–6. The target was sufficiently thin so that multiple scattering of

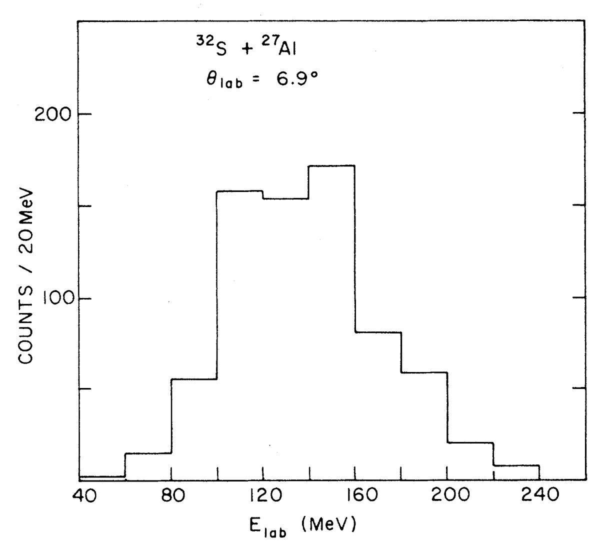

FIG. 3. Energy spectrum for evaporation residues following complete fusion of 336-MeV ^{32}S and ^{27}Al at θ_{lab} = 6.9°, which is near the peak in the $d\sigma/d\theta$ distribution.

the products will have the largest effect on the large-angle tails of these distributions but should be of little significance for the most probable angle and the distribution about that angle. In determining an angle-integrated cross section (σ_{er}), it is convenient to graphically find the area under the curve $d\sigma/d\theta$ vs θ. Such curves must pass through the origin since $d\sigma/d\theta = 2\pi \sin\theta(d\sigma/d\Omega)$. As is apparent from the example in Fig. 7, any reasonable extrapolation to $\theta = 0$ will result in the same area to within a few percent. The evaporation-residue cross sections obtained in the present work are listed in Table I along with corresponding values for l_{cr}, σ_{er}/σ_R, and the peak of the Z distribution (Z_{max}).

III. COMPARISON TO MICA RESULTS

The values for σ_{er} measured here with a counter telescope are from 1.5–2.5 times larger than the mica results of KJM[1] for bombardments with 168-MeV ^{16}O and both 210- and 138-MeV ^{20}Ne (see Table I). We believe these discrepancies arise because a significant number of evaporation residues have sufficiently low atomic numbers and high kinetic energies to escape detection in mica. Better agreement with the mica data was obtained for the lower energy ^{16}O bombardments, where kinetic energies are lower and atomic numbers are higher.

An underlying assumption in the work of Ref. 1 was that a conventional evaporation calculation would predict a fairly accurate Z distribution for the evaporation residues. However, such is not the case for high bombarding energies, as can be seen by comparing the experimental Z distribution for 210-MeV ^{20}Ne + ^{27}Al with one calculated by the method of Dostrovsky, Fraenkel, and Friedlander[7] (DFF) (Fig. 8). The DFF distribution is repre-

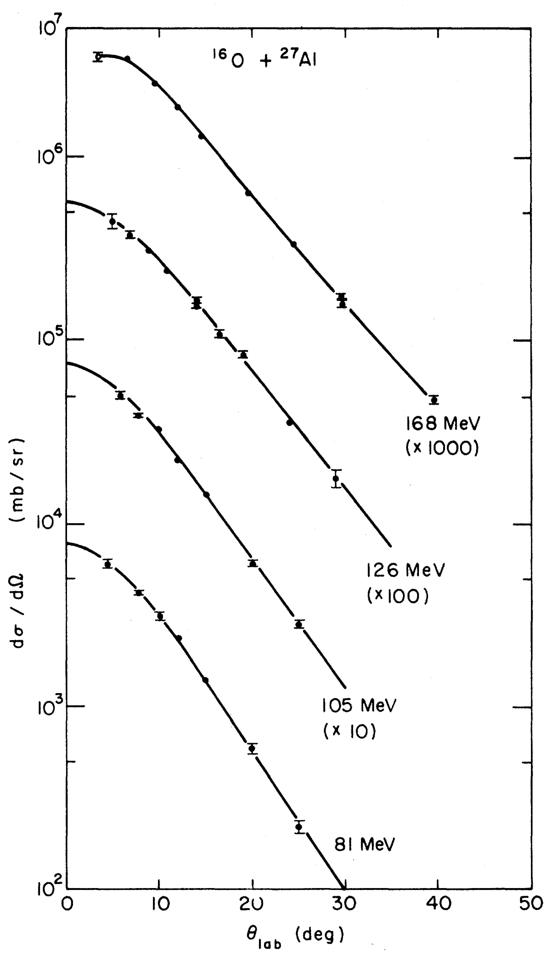

FIG. 4. Angular distributions for evaporation residues following complete fusion of ^{16}O and ^{27}Al. The curves are drawn to guide the eye.

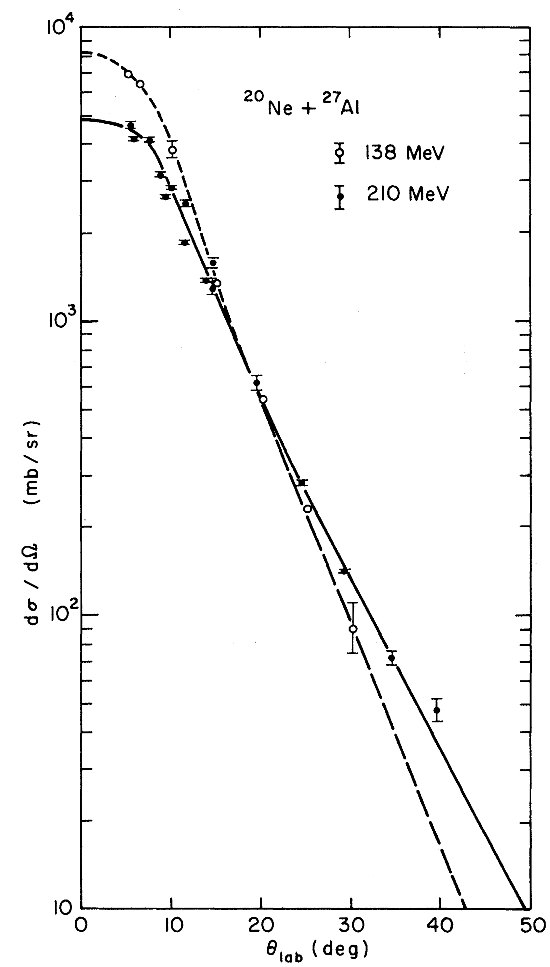

FIG. 5. Angular distributions for evaporation residues following complete fusion of ^{20}Ne and ^{27}Al. The curves are drawn to guide the eye.

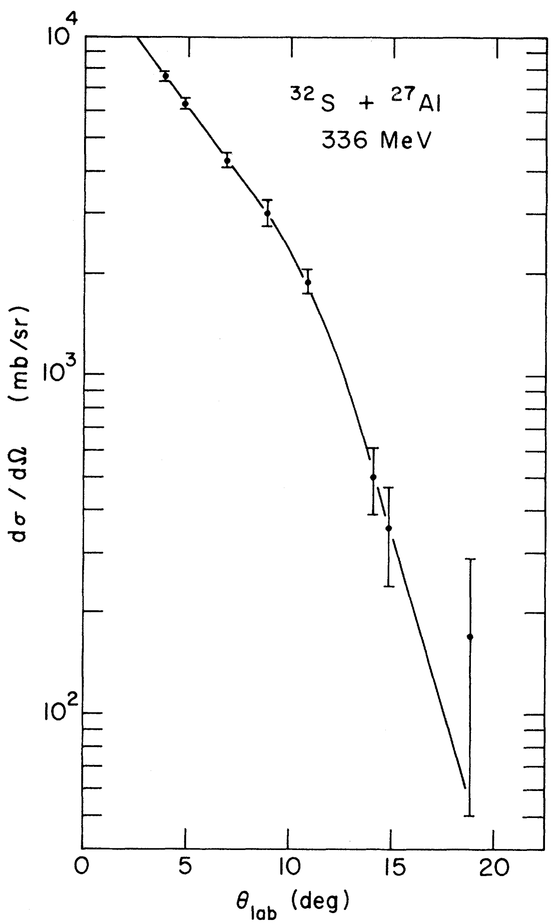

FIG. 6. Angular distribution for evaporation residues following complete fusion of 336-MeV ^{32}S and ^{27}Al. The curve is drawn to guide the eye.

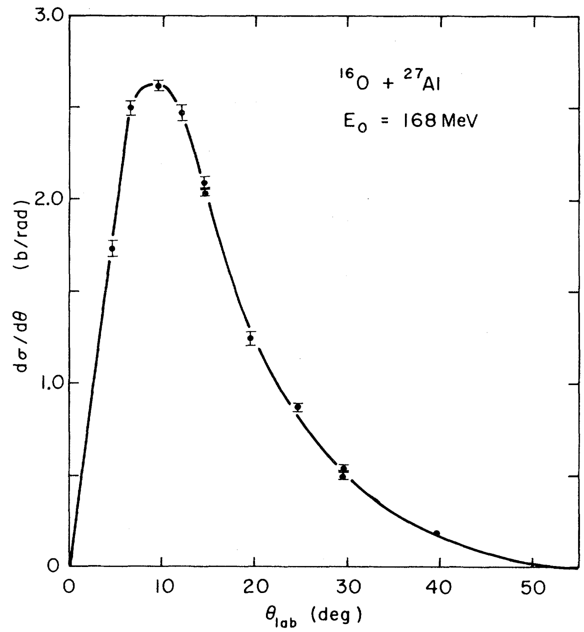

FIG. 7. Angular distribution expressed as $d\sigma/d\theta$ vs θ for evaporation residues following the complete fusion of 168-MeV ^{16}O and ^{27}Al.

sented as a dashed line. The experimental distribution is just a spectrum from the ΔE detector over a narrow range of $(E\text{-}\Delta E)$ near θ_{max}, and examination of entire $\Delta E-(E\text{-}\Delta E)$ matrices suggests this spectrum is a reasonably good representation of the over-all Z distribution. For 210-MeV $^{20}Ne + ^{27}Al$, the kinetic energies of the evaporation residues are such that the majority having $Z \lesssim 16$ would probably not be detectable using mica.[8] Thus, one can easily account for

TABLE I. Summary of results for complete fusion of heavy ions with Al.

Reaction	E_{lab} (MeV)	σ_{er} (mb) Mica[b]	Counters[c]	σ_{er}/σ_R [c,d]	l_{cr}[a] Exp.[c]	Friction[e]	Fission limit[f]	Z_{max} [c,g]
$^{16}O + ^{27}Al$	81	1550± 250	1020± 150	0.77	27± 2			18
	105	1200± 180	1040± 120	0.67	31± 2	32–34	33	17
	126	815± 120	960± 120	0.58	33± 2		33.5	16
	168	500± 100	860± 110	0.48	36± 2	38–40	35	14
$^{20}Ne + ^{27}Al$	138	600± 120	1170± 130	0.71	40± 2		36	18
	210	380± 100	940± 150	0.55	44± 4	46–48	39	16
$^{32}S + ^{27}Al$	336		620± 80	0.33	46± 3			22

[a] Critical value of entrance channel angular momentum for evaporation residues. Values for friction are for all of complete fusion, including fission.
[b] See Ref. 1, where it was assumed that $\sigma_{er} = \sigma_{cf}$.
[c] Present work.
[d] Calculated using σ_R values from Refs. 1 and 6.
[e] See Ref. 9.
[f] See Ref. 10.
[g] Most probable Z for evaporation residues.

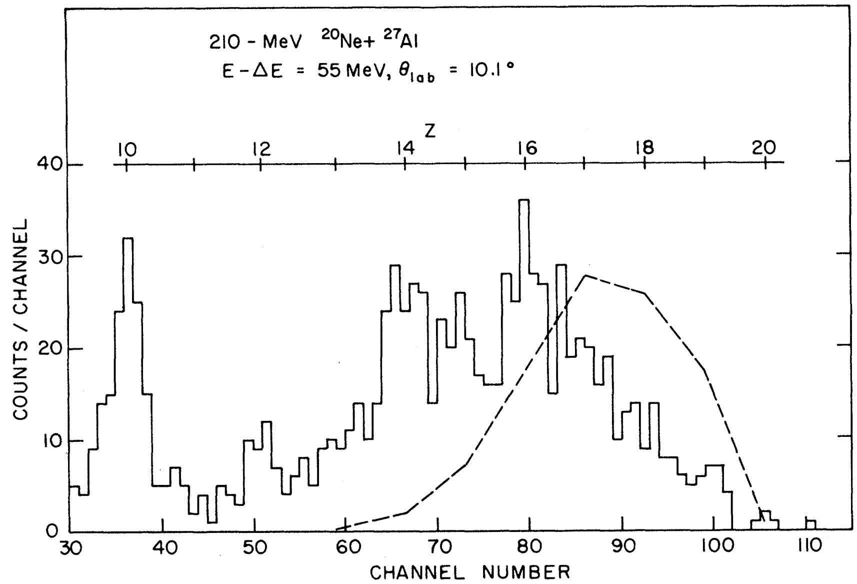

FIG. 8. Spectrum from ΔE detector for a narrow range of $(E\text{-}\Delta E)$ showing elemental distribution of evaporation residues for 210-MeV ^{20}Ne + ^{27}Al. The distribution predicted by a Monte Carlo cascade calculation (Ref. 7) is shown by the dashed curve.

the large discrepancies between the counter telescope and mica detectors at high energies. (It should be noted that the 100% efficiency thresholds of Ref. 8 supersede the higher-energy values indicated in Fig. 1 of Ref. 1.) The shifting of the Z distribution undoubtedly occurs because the compound nuclei have large angular momenta which cause a large fraction of them to emit particles larger than nucleons while decaying. Thus, the evaporation residues have lower atomic numbers than those predicted by the DFF calculation since the calculation does not account for these angular momentum effects. Such effects are not so important at lower bombarding energies, as is shown by a comparison of the DFF Z distribution with the experimental one for the 81-MeV ^{16}O + ^{27}Al

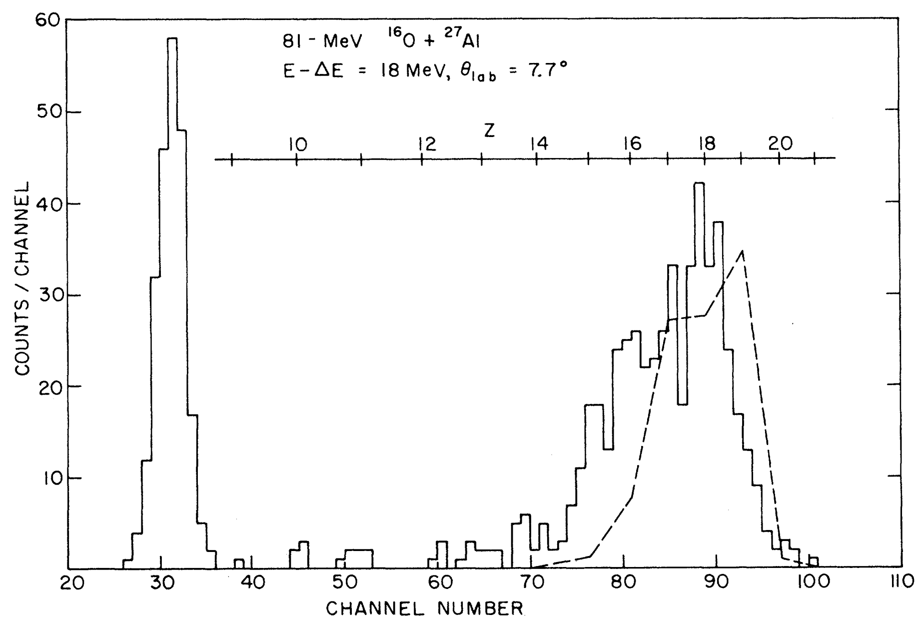

FIG. 9. Spectrum from ΔE detector for a narrow range of $(E\text{-}\Delta E)$ showing elemental distribution of evaporation residues for 81-MeV ^{16}O + ^{27}Al. See also Fig. 8 caption.

system (Fig. 9), and better agreement with mica results is obtained (Table I).

IV. INTERPRETATION AND DISCUSSION

The cross section for complete fusion can be written as

$$\sigma_{cf} = \pi \lambda\!\!\!^{-2} \sum_{l=0}^{\infty} (2l+1) P_l \ . \qquad (1)$$

In the sharp cutoff approximation, where the fusion probabilities (P_l) are unity for $l \leq l_{cr}$ and zero otherwise,

$$\sigma_{cf} = \pi \lambda\!\!\!^{-2} \sum_{l=0}^{l_{cr}} (2l+1) = \frac{\pi \hbar^2}{2\mu E}(l_{cr}+1)^2 \ , \qquad (2)$$

where E is the initial kinetic energy in the center of mass. Values of l_{cr} obtained in the present work (assuming $\sigma_{er} = \sigma_{cf}$) are listed in Table I and are seen to be in good agreement with calculations by Gross and Kalinowski,[9] who employ anisotropic friction to describe the dynamics of heavy ion collisions. Our results for $^{16}O + {}^{27}Al$ are also in good agreement with those of Plasil and Blann[10] who calculate l_{cr} for evaporation residues under the condition that fission is allowed to compete in the decay of the compound nucleus. For the $^{20}Ne + {}^{27}Al$ system, the experimental results are somewhat higher than the calculations of Ref. 10.

If it is assumed that none of the relative energy or angular momentum is dissipated into excitations in the approach trajectory, one may write

$$E = V(R_{cr}) + \frac{\hbar^2}{2I} l_{cr}(l_{cr}+1) \approx V(R_{cr}) + \frac{\hbar^2}{2I}(l_{cr}+1)^2 \ . \qquad (3)$$

Here, $V(R_{cr})$ contains both nuclear and Coulomb terms; R_{cr} is the classical turning radius for angular momentum l_{cr}; and presumably the maximum separation for which complete fusion can occur. Using μR_{cr}^2 for the moment of inertia (I) and eliminating l_{cr} between Eqs. (2) and (3) yields

$$\sigma_{cf} \approx \pi R_{cr}^2 \left(1 - \frac{V(R_{cr})}{E}\right) \ . \qquad (4)$$

Equation (4) may be used as an aid to interpret complete-fusion data for energies well above the fusion barrier, in which case R_{cr} and $V(R_{cr})$ should reflect properties of the nuclear interior. Most of the present work is in this category. For energies not far above the fusion barrier, essentially all of the reaction cross section is contained in σ_{cf}, so l_{cr} in Eqs. (2) and (3) is replaced by l_{max}, the maximum l value for which reactions occur. In such cases, it follows that

$$\sigma_{cf} = \pi R_B^2 \left(1 - \frac{V(R_B)}{E}\right) \qquad (5)$$

which is identical in form to Eq. (4), but the parameters R_B and $V(R_B)$ now refer to the radial position and height of the fusion barrier.

For $V(R_{cr}) < V(R_B)$, which is usually the case, σ_{cf} is governed by Eq. (5) up to the energy at which the combined fusion and angular momentum barrier at R_B is surpassed by the corresponding quantity at R_{cr}. For higher energies, Eq. (4) becomes operative. If the fusion barrier is low enough so that $V(R_{cr}) > V(R_B)$, σ_{cf} is always described by Eq. (4). A detailed discussion of the variation of σ_{cf} over a wide range of energies is given by Glas and Mosel.[11]

Calculations of $r_{cr} = R_{cr}/(A_1^{1/3} + A_2^{1/3})$, using Eq. (3) with existing complete-fusion data for l_{cr} along with potentials obtained from Brueckner theory in the "sudden approximation" for V, were performed by Galin *et al.*[12] for a wide range of nuclear systems and energies. In the sudden approximation, it is assumed that both nuclei retain their ground-state density distributions, i.e., they suffer no distortions until fusion occurs. It

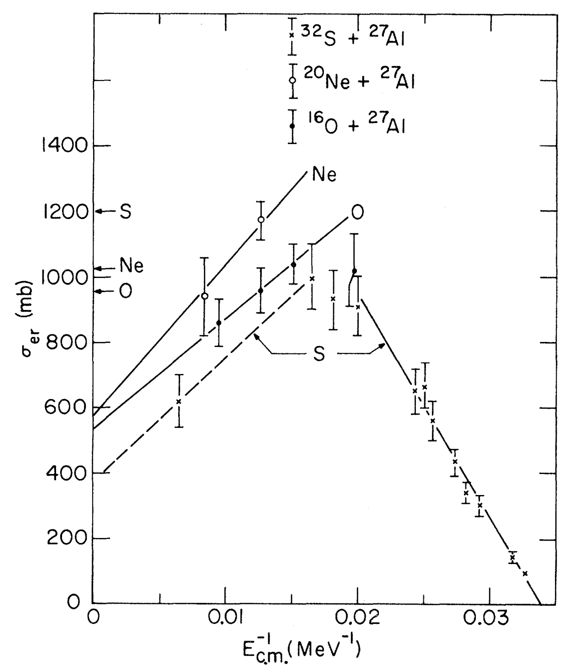

FIG. 10. Plot of evaporation residue cross sections from the present work and the $^{32}S + {}^{27}Al$ cross sections of Ref. 3 vs $1/E$ [see Eqs. (4) and (5) in text]. The straight line of negative slope through most of the data of Ref. 3 corresponds to $r_B = R_B/(32^{1/3} + 27^{1/3}) = 1.4$ fm and $V(R_B) = 29.7$ MeV [Eq. (5) in text]. The Ne and O lines have ordinate intercepts corresponding to $r_{cr} = 0.75$ fm [Eq. (4)]. Intercepts for $r_{cr} = 1.0$ fm are indicated by arrows. Errors shown for Ne and O data are relative and do not include systematic errors common to all data points. Absolute errors are shown for the S+Al data.

TABLE II. Critical radius parameters and potentials for complete fusion.

Reaction	r_{cr} (fm) [a] Upper limit	Best value	$V(R_{cr})$ [b] (MeV) Best R_{cr}	$r_{cr}=0.75$ fm
$^{16}O+^{27}Al$	0.95	0.76	−55	−61
$^{20}Ne+^{27}Al$	0.98	0.69	−110	−80
$^{32}S+^{27}Al$	0.69	0.56	−100	

[a] $r_{cr} \equiv R_{cr}/(A_1^{1/3}+A_2^{1/3})$.
[b] Includes Coulomb and nuclear potentials. See text Sec. IV and Fig. 10 for details.

was found that r_{cr} was nearly constant at about 1.0 fm over much of the Periodic Table. We performed calculations using a potential similar to that of Ref. 12 for our $^{16}O+^{27}Al$ data and obtained values for r_{cr} in the range 1.0–1.1 fm. Unfortunately, the critical radius obtained in this way is strongly dependent on the parameters used in the potential and, as will be seen shortly, the above results are not consistent with the general trend of our experimental data.

A value for the critical radius can be obtained independently of any assumptions about the potential if a plot of σ_{cf} vs $1/E$ is a straight line for a given projectile-target system [see Eq. (4)]. Such a plot for the data of the present work and the $^{32}S+^{27}Al$ data of GWB[3] is shown in Fig. 10. It appears from the data presented in that figure that the dependence of σ_{er} on E^{-1} might be described by two straight lines for a given system, one for high energies ($E^{-1} \lesssim 0.015$ MeV^{-1}) [Eq. (4)] and one for low energies ($E^{-1} \gtrsim 0.02$ MeV^{-1}) [Eq. (5)]. If this assumption is made for high energies, the r_{cr} values obtained from the ordinate intercepts are 0.76 and 0.69 fm for the $^{16}O+^{27}Al$ and $^{20}Ne+^{27}Al$ systems, respectively, with upper limits of approximately 1 fm for each (see Table II). A value of 0.56 fm is obtained for the $^{32}S+^{27}Al$ system if one joins the GWB data point at highest energy with the one from the present work (dashed line in Fig. 10). The solid lines labeled Ne and O in Fig. 10 both have intercepts corresponding to $r_{cr}=0.75$ fm. The arrows indicate the ordinate locations for $r_{cr}=1.0$ fm, which would correspond roughly to the intercepts for the potential of Ref. 12.

The critical radius parameters deduced above are considerably smaller than those of Galin *et al.*[12] Also, the values for $V(R_{cr})$ range from −55 to −110 MeV, which would correspond to deep attractive potentials. The r_{cr} value for the $^{32}S+^{27}Al$ system is exceptionally small, although it is not clear whether either of the data points used is in a straight line region of σ_{cf} vs $1/E$. Complete-fusion measurements for this system at some intermediate energies are needed to settle this question.

The values of r_{cr} listed in Table II should correspond to a considerable overlap and/or distortion of nuclear matter. Under such conditions, the validity of the sudden approximation and the validity of Eqs. (3) and (4) is certainly questionable. A more realistic treatment of the problem would include deformations and loss of energy and angular momentum in the entrance channel, in which case the relation between σ_{cf}, R_{cr}, $V(R_{cr})$, and E would undoubtedly be more complex than implied by Eq. (4). If the dissipating forces are represented as ordinary friction, the calculations of Gross and Kalinowski[9] for the $^{12}C+^{27}Al$ system at high energies indicate σ_{cf} is still a linear function of $1/E$, but it is not clear whether this is indicative of a constant R_{cr}. In fact, there are also indications that this friction representation may be invalid for such light projectile-target combinations as those of the present work.[13] In any case, the positive slope of σ_{cf} vs $1/E$ suggests, at this level of approximation, that the effective potential for the colliding nuclei is attractive and possibly quite deep at the fusion radii for high bombarding energies. More measurements of $\sigma_{cf}(E)$ are required, however, before its true functional form can be firmly established. This, in addition to more theoretical work, is necessary before conclusions can be drawn concerning critical radius parameters for fusion.

V. SUMMARY AND CONCLUSIONS

A comparison of the counter-telescope measurements of complete-fusion cross sections with those using mica track detectors has shown that, for light nuclear systems at high bombarding energies, measurements with mica detectors should be approached with caution. The problem appears to be one of nonregistration in mica due to a combination of low Z and high kinetic energies for some of the evaporation residues. The low atomic numbers are most probably the consequence of angular-momentum-enhanced emission of heavy particles. At lower bombarding energies, where atomic numbers are higher and kinetic energies are lower, the counter telescope and mica results are in fair agreement.

A critical radius for complete fusion might be estimated from the intercept of a straight line drawn through the data plotted as σ_{cf} vs $1/E$ (Fig. 10). In the present work, the radii so deduced are smaller and the associated potentials are much more attractive than expected from the sudden approximation. It therefore appears that some mechanism for deformation and/or energy dissipation in the entrance channel must be included in considering the concept of a constant critical radius parameter. The generally small r_{cr} values may be partially due to the nuclear structure effects discussed by Glas and Mosel,[14] since all of our bombarding projectiles are α-conjugate nuclei whose single-particle separation energies are relatively high. Clearly, many more experimental cross sections are needed, and measurements for the $^{32}S + ^{27}Al$ system at energies between 132.5 MeV (Ref. 3) and 336 MeV (present work) are of immediate interest.

The authors wish to thank the staff of the Yale heavy ion accelerator for their assistance and cooperation.

---

†Work supported by the U.S. Atomic Energy Commission.
*Present address: Department of Physics, Queen's University, Kingston, Ontario, Canada K7L3N6.

[1]L. Kowalski, J. C. Jodogne, and J. M. Miller, Phys. Rev. 169, 894 (1968).
[2]J. B. Natowitz, E. T. Chulick, and M. N. Namboodiri, Phys. Rev. C 6, 2133 (1972).
[3]H. H. Gutbrod, W. G. Winn, and M. Blann, Nucl. Phys. A213, 267 (1973).
[4]R. L. Kozub, J. M. Miller, K. Kowalski, D. Logan, and N. H. Lu, in *Proceedings of the International Conference on Reactions Between Complex Nuclei*, edited by R. L. Robinson *et al.* (North-Holland, Amsterdam, 1974), p. 112.
[5]Manufactured by Union Carbide Corporation.
[6]B. Wilkens and G. Igo, in *Proceedings of the Third International Conference on Reactions Between Complex Nuclei* (Univ. California Press, Berkeley, 1963), p. 241.
[7]I. Dostrovsky, Z. Fraenkel, and G. Friedlander, Phys. Rev. 116, 683 (1960); 119, 2098 (1960).
[8]P. B. Price and R. L. Fleischer, Annu. Rev. Nucl. Sci. 21, 295 (1971).
[9]D. H. E. Gross and H. Kalinowski, Phys. Lett. 48B, 302 (1974).
[10]F. Plasil and M. Blann, unpublished.
[11]D. Glas and U. Mosel, in *Proceedings of the International Conference on Reactions Between Complex Nuclei*, edited by R. L. Robinson *et al.* (see Ref. 4), p. 123.
[12]J. Galin, D. Guerreau, M. Lefort, and X. Tarrago, Phys. Rev. C 9, 1018 (1974). See also, R. Basile, J. Galin, D. Guerreau, M. Lefort, and X. Tarrago, J. Phys. (Paris) 33, 9 (1972).
[13]R. Beck and D. H. E. Gross, Phys. Lett. 47B, 143 (1973).
[14]D. Glas and U. Mosel, Phys. Lett. 49B, 301 (1974).